World Academy of Science, Engineering and Technology
International Journal of Civil and Environmental Engineering
Vol:13, No:9, 2019

Influence of Concrete Cracking in the Tensile Strength of Cast-in Headed Anchors

W. Nataniel, B. Lima, J. Manoel, M. P. Filho, H. Marcos, Oliveira Mauricio, P. Ferreira

***Abstract*—**Headed reinforcement bars are increasingly used for anchorage in concrete structures. Applications include connections in composite steel-concrete structures, such as beam-column joints, in several strengthening situations as well as in more traditional uses in cast-in-place and precast structural systems. This paper investigates the reduction in the ultimate tensile capacity of embedded cast-in headed anchors due to concrete cracking. A series of nine laboratory tests are carried out to evaluate the influence of cracking on the concrete breakout strength in tension. The experimental results show that cracking affects both the resistance and load-slip response of the headed bar anchors. The strengths measured in these tests are compared to theoretical resistances calculated following the recommendations presented by fib Bulletin no. 58 (2011), ETAG 001 (2010) and ACI 318 (2014). The influences of parameters such as the effective embedment depth (h_{ef}), bar diameter (d_s), and the concrete compressive strength (f_c) are analysed and discussed. The theoretical recommendations are shown to be over-conservative for both embedment depths and were, in general, inaccurate in comparison to the experimental trends. The ACI 318 (2014) was the design code which presented the best performance regarding to the predictions of the ultimate load, with an average of 1.42 for the ratio between the experimental and estimated strengths, standard deviation of 0.36, and coefficient of variation equal to 0.25.

***Keywords*—**Cast-in headed anchors, concrete cone failure, uncracked concrete, cracked concrete.

I. Introduction

CAST-IN headed bars are increasingly used to transfer forces in precast and cast-in-place concrete structures. Their use simplifies the structural detailing, boost the construction process, favoring structural flexibility and economy. They are widely used to connect different structural members, e.g. in base-column joints and beam-column connections as well as in several strengthening situations. In these cases, the overall strength of the structure ordinarily depends on the concrete cone resistance. Reference [8] states that this failure mode is characterized by a circumferential crack with a conical shape that starts in the anchor's head and spreads steadily until failure.

The experimental and numerical evidences available on literature show that besides essential variables such as the effective embedment depth of the anchor (h_{ef}), or the concrete compressive strength (f_c), the cracking state of the structure affects the anchorage resistance. According to [11], the failure load of headed anchors failing by concrete cone breakout is reduced by nearly 25% for a crack width of 0.3 mm. Besides, [6] states that experimental data showed that the average concrete cone resistance in cracked zones could be reasonably assumed as about 70% of their capacity in uncracked structural elements. According to [5], [7], the decreasing of approximately 30% in the concrete cone resistance due to concrete cracking can be linked to a reduction on the intensity of the transferred forces close to the crack plane (see Fig. 1). This change in the distribution of the reaction force, which becomes non-uniform and more concentrated at the edges, as shown in Fig. 1, is caused by the reduction of stiffness parallel to the direction of the crack. References [2]-[4] also show that the concrete cone capacity can be greatly affected by the presence of cracks in concrete.

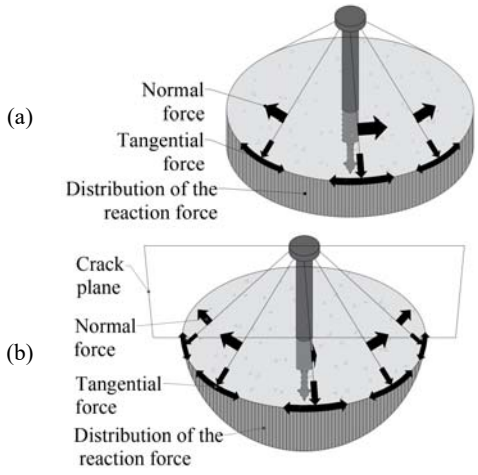

Fig. 1 Influence of crack on the load transfer mechanisms. (a) uncracked concrete, (b) cracked concrete (adapted from [5])

This paper presents and discusses the results of nine pull-out tests performed on single cast-in headed anchors embedded in reinforced concrete elements. These tests were carried to investigate the influence of concrete cracking on the ultimate tensile capacity of the headed steel anchors. The cracking width was varied on these tests as a function of the flexural reinforcement ratio of the reinforced concrete specimens. The overall behavior and ultimate resistances are presented and used to evaluate the performance of the design equations presented by [1], [9], [10].

II. Methods of Calculation

The ultimate tensile capacity of single cast-in headed

N. W.*, B. Lima, M. J., M. P. Filho, and M. H. Oliveira are with the Department of Civil and Environmental Engineering, University of Brasilia, Brasilia, FD Brazil (*corresponding author, phone: +55 88 99360-8826; e-mail: nwontoon@gmail.com).

M. P. Ferreira is with the Faculty of Civil Engineering, Institute of Technology, Federal University of Para, Para, Brazil (e-mail: mpinaf@gmail.com).

anchors without edge and spacing effects to concrete cone failure is usually calculated on the basis of expressions as presented in (1), where k_1 is a constant that accounts for the cracking state of concrete, f_c is the compressive strength of concrete, and h_{ef} is the effective embedment depth of the anchor. Table I summarizes the most important theoretical parameters assumed in [1], [9], [10].

$$N_t = k_1 \cdot \sqrt{f_c} \cdot h_{ef}^{\,n} \quad (1)$$

III. Experimental Program

The tested specimens were idealized to represent local models of semi-rigid beam-column joints as shown in Fig. 2. The highlighted rectangular area represents the concrete prisms where the headed anchors were embedded. In real structural situations, these regions may or may not be cracked, depending on the combination of loads and bending moments being transferred in the connection. All tests were designed to fail by concrete cone breakout.

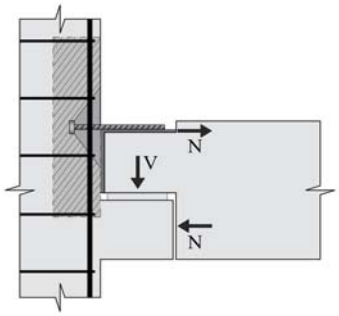

Fig. 2 Headed anchors in precast concrete beam-column joints

This series of tests aimed to evaluate the influence of concrete cracking in the ultimate tensile capacity of single cast-in headed anchors in tension. The headed studs were embedded in reinforced concrete specimens 350 mm wide (b_w), 200 mm thick (h) and 900 mm long (L), and they were fabricated with a head diameter (d_h) three times larger than the diameter of the shanks (d_s). The main variables were the diameter of the anchors, 10 mm and 16 mm, the effective embedment length of the anchors, 60 mm and 110 mm, and the flexural reinforcement ratio (ρ_f) of the reinforced concrete specimens, which was used as crack control reinforcement. For embedment lengths of 60 mm, ρ_f varied from 0.13% to 1.24%, and for embedment lengths of 110 mm, it ranged from 0.33% to 3.21%.

The concrete was made with Portland cement CP-II-Z-32 (with 6% to 14% of pozzolan addition), natural sand, and rolled pebble with a maximum diameter of 9.5 mm as coarse aggregate. Tested specimens were wet cured for 7 days, and their main characteristics are summarized in Table II. Fig. 3 presents details of their reinforcement.

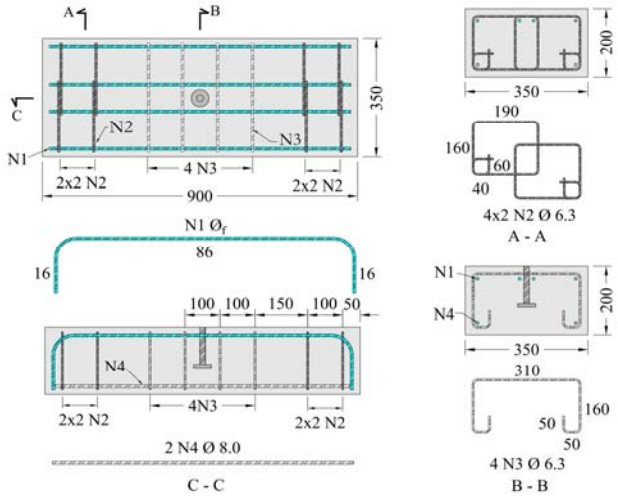

Fig. 3 Detailing of the specimens' reinforcement

The mechanical properties of concrete were determined from tests on concrete cylindrical samples following the recommendations of Brazilian standards. The compressive and tensile strength of concrete were obtained from tests on 100 mm x 200 mm cylinders, carried on the same day of the pull-out tests. The modulus of elasticity was determined through tests on 150mm x 300mm samples. The mean values were: f_{cm} = 34.5 MPa, f_{ctm} = 1.5 MPa, E_c = 23.5 GPa. The headed anchors were submitted to uniaxial tension tests to determine the steel mechanical properties and they showed an elastic-plastic response. These results are also summarised in Table II.

Vertical displacements were measured by dial gauges (DG) as indicated in Fig. 3. DG_1 measured the vertical displacement of the reinforced concrete specimen and DG_2 was attached to the stud's head through a hole located in the lower surface of the concrete prism, allowing the assessment of anchors' slip. The position of the strain gauges in the shank (G_s) and close to the stud's head (G_h) as well as those positioned to monitor strains in the flexural reinforcement (G_f) are also shown in Fig. 4.

TABLE I
Definition of Theoretical Parameters

Symbols	Parameter	*fib* Bull. 58	ETAG 001	ACI 318
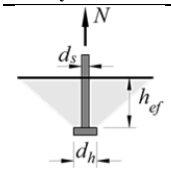	k_1 for uncracked concrete	12.7	10.1	12.5 for $h_{ef} < 280$ mm 4.9 for 280 mm $\le h_{ef} < 635$ mm
	k_1 for cracked concrete	8.9	7.2	10 for $h_{ef} < 280$ mm 3.9 for 280 mm $\le h_{ef} < 635$ mm
	n	3/2	3/2	3/2 for $h_{ef} < 280$ mm 5/3 for 280 mm $\le h_{ef} < 635$ mm

TABLE II
CHARACTERISTICS OF TESTED SPECIMENS

Specimens	Headed steel anchors						Flexural reinforcement				
	h_{ef} (mm)	d_s (mm)	d_h (mm)	f_{ya} (MPa)	E_{sa} (GPa)	d (mm)	N1ϕ_f	ϕ_f (mm)	f_{ys} (MPa)	E_{sa} (GPa)	ρ_f (%)
F-60-0.1	61	10	30	504	190	171	4	6.3	544	198	0.13
F-60-0.3	63					172	4	8.0	580	196	0.33
F-60-0.5	62					170	4	10.0	504	190	0.53
F-60-1.2	60					170	6	12.5	515	191	1.24
F-110-0.3	116	16	51	545	190	175	4	8.0	580	196	0.33
F-110-0.5	114					176	4	10.0	504	190	0.51
F-110- 0.8	115					176	4	12.5	515	191	0.80
F-110- 1.6	116					166	8	12.5			1.69
F-110- 3.2	113					168	6	20.0	546	194	3.21

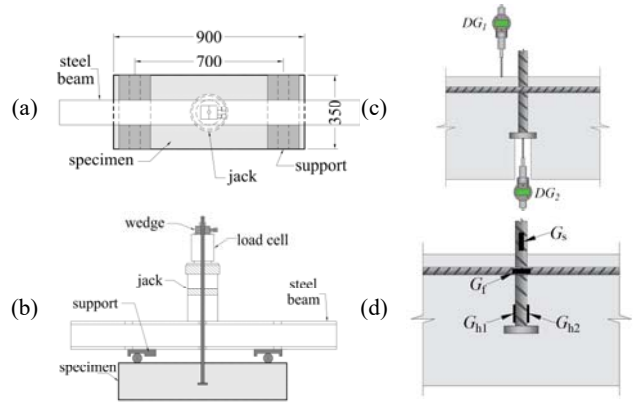

Fig. 4 Tests setup and instrumentation. (a) plain view, (b) side view, (c) dial gauges, (d) strain gauges

IV. RESULTS AND DISCUSSIONS

All the tested specimens failed due to concrete cone failure. Fig. 5 summarises the experimental responses of the specimens of the F-110 series, which reflect in a bigger scale the results observed on those from the F-60 series. As expected, the larger flexural reinforcement ratio resulted in stiffer load-displacement responses (see Fig. 5 (a)) and smaller strains in the flexural reinforcement (see Fig. 5 (b)), reducing the width of the cracks effectively.

These tests confirm the observations presented by [5] that the cracking state and width affect the load-slip response of the cast-in headed anchors as shown in Fig. 5 (c). It is possible to see that up to a tensile load of 30 kN, which is the predicted cracking load for these specimens, the load-slip response of all anchors was almost the same. Then, the specimens with the lowest values of ρ_f (F-110-0.3; F-110-0.5; F-110-0.8) showed larger slip increments while the others (F- 110-1.7 and F-110-3.2) showed stiffer response up to a loading level where the increase in the flexural rebars' strain allowed the anchors' slip.

Fig. 6 (a) shows the relationship observed between the strains in the shank of the headed anchors outside the concrete prism (G_s) and inside, close to the anchors' head (G_h). These results refer to specimen F-110-0.5, but reflect what was observed in the others. Strains close to the stud's head inside the concrete prism were shown to be almost equal to those on the outside, evidencing that the interlock between the stud's head and concrete is the main anchorage mechanism in the case of the performed experiments. The axial tensile force and the measured strains in the shank of the anchors are presented in Figs. 6 (b) and (c). It is shown that the load carrying capacity of the anchors is significantly affected by the cracking state once the anchors embedded in the specimens with the higher flexural reinforcement ratio yielded before the concrete cone failure.

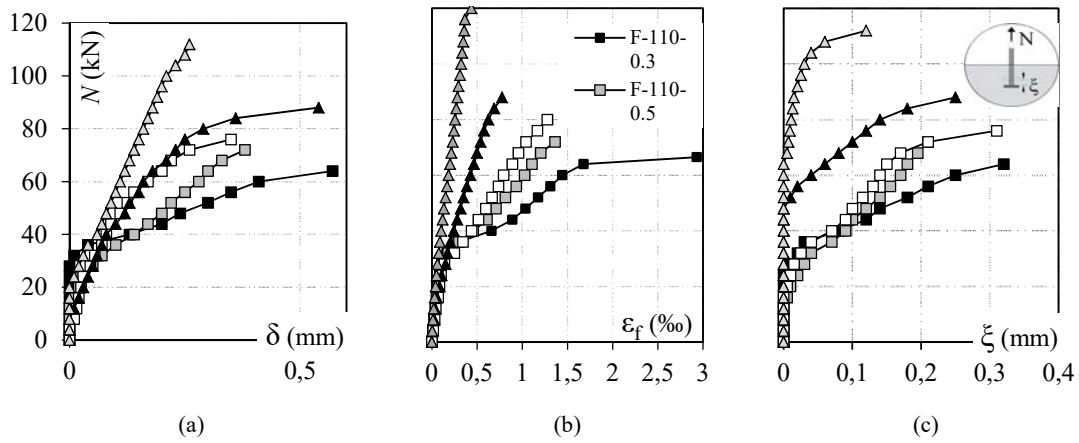

Fig. 5 Experimental response of F-110 series. (a) Load-displacement curves. (b) Load-strains curves in the flexural rebars. (c) Load-slip curves

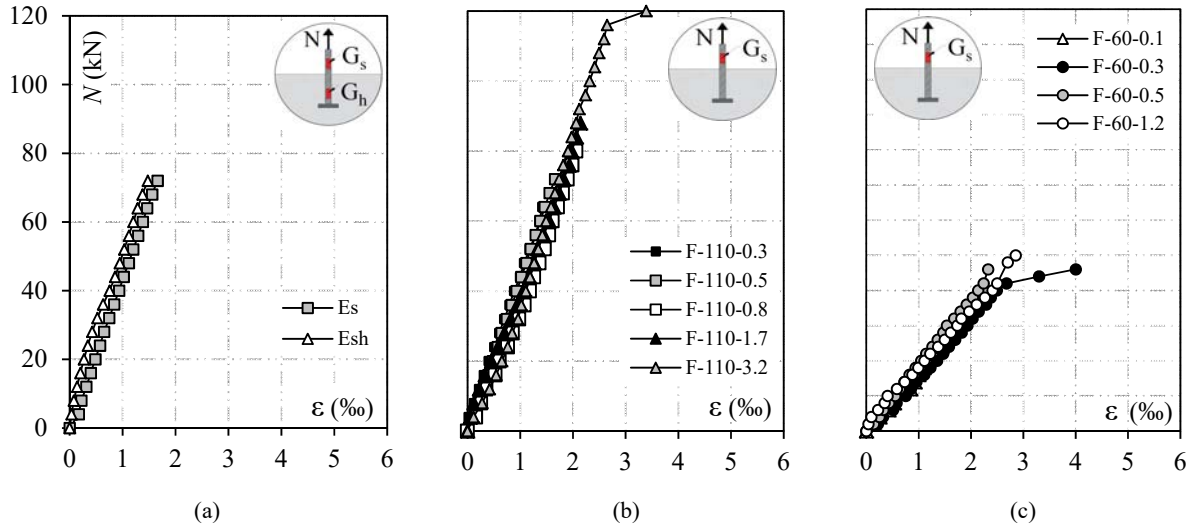

Fig. 6 Load-strain curves. (a) Comparison of strains on the shank (G_s) and close to the anchor's head (G_h) for specimen F-110-0.5. (b) and (c) Load-strains in the anchors (G_s) for series F-100 and F-60

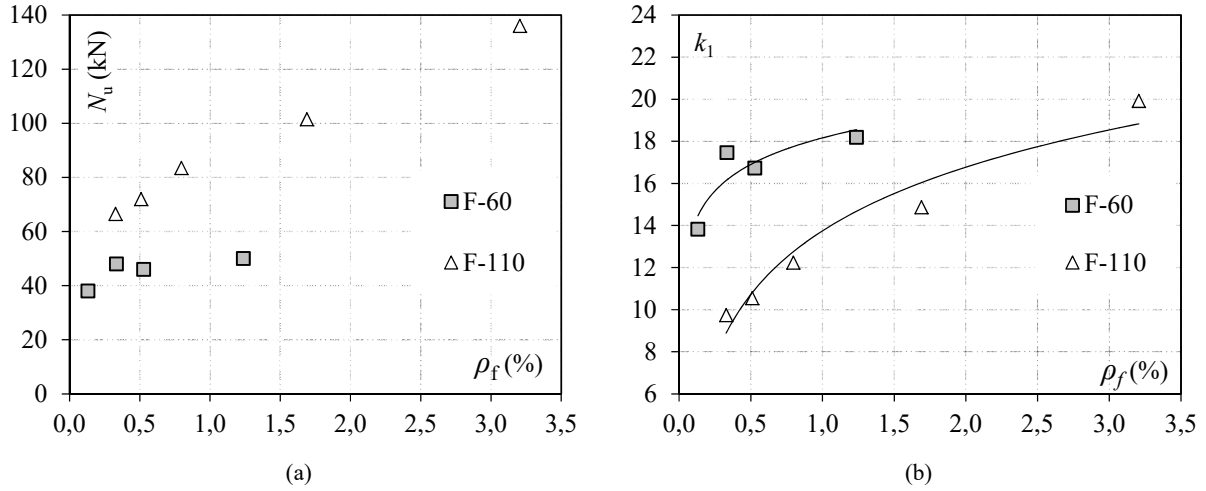

Fig. 7 Experimental strengths. (a) Relationship between ultimate loads and flexural reinforcement. (b) k_1 factor as a function of flexural reinforcement

TABLE III
SUMMARY OF THE RESULTS

Specimens	h_{ef} (mm)	ρ_{flex} (%)	N_u (kN)	$N_u/N_{fib,cr}$	$N_u/N_{ETAG,cr}$	$N_u/N_{ACI,cr}$
F-60-0.1	61	0.13	38.0	1.53	1.89	1.36
F-60-0.3	63	0.33	48.0	1.84	2.27	1.63
F-60-0.5	62	0.53	46.0	1.80	2.23	1.60
F-60-1.2	60	1.24	50.0	2.06	2.54	1.83
F-110-0.3	116	0.33	66.5	1.02	1.26	0.91
F-110-0.5	114	0.51	72.0	1.13	1.40	1.01
F-110-0.8	115	0.80	83.5	1.30	1.60	1.15
F-110-1.7	116	1.69	101.5	1.55	1.60	1.40
F-110-3.2	113	3.21	136.0	2.17	2.68	1.93
	Ave.			1.60	1.94	1.42
	S.D.			0.40	0.51	0.36
	C.V.			0.25	0.26	0.25

Fig. 7 (a) shows the ultimate tensile capacity (N_u) measured on tests as a function of the flexural reinforcement ratio. This figure shows that for both values of effective embedment depth (60 mm and 110 mm) the load carrying capacity of the anchors increased with increments of the flexural reinforcement ratio of the reinforced concrete members where

they were embedded. In Fig. 7 (b), the k_1 factor obtained in these tests, taken as (N_u / $f_c^{0.5}$ · $h_{ef}^{1.5}$), is presented as a function of the flexural reinforcement ratio. For both embedment lengths, it can be observed that the k_1 factor grows as the flexural reinforcement increases, also showing that the theoretical values assumed in the design methods presented above are conservative, especially for uncracked concrete.

Table III compares the ultimate tensile capacity (N_u) with the values theoretically calculated following the provisions of fib Bulletin 58 (2011), ETAG 001 Annex C (2010) and [1]. The theoretical estimates tended to diverge from the experimental results as the flexural reinforcement ratio increased. Among the theoretical methods analysed, [1] showed the best correlation with the experimental tests performed in this research. Reference [1] had an average value between N_u/N_{theo} of 1.42 and presented the lower standard deviation (0.36) and coefficient of variation (0.25). None of the methods was able to predict correctly the exponential influence of the flexural reinforcement ratio in the load carrying capacity of the headed anchors embedded in reinforced concrete members.

V. Conclusions

This paper presents the results of nine tests on cast-in headed anchors embedded in reinforced concrete members under tensile axial loads. The main variables in these tests were the diameter of the anchors, the effective embedment length, and the flexural reinforcement ratio of the reinforced concrete specimens. The measured ultimate tensile capacity was compared to theoretical predictions calculated using fib Bulletin no. 58 (2011), ETAG 001 Annex C (2010) and [1]. The main conclusions were:

I. Larger crack widths observed in specimens with lower flexural reinforcement ratios favoured premature slipping of the headed anchors under tension;
II. Failure loads of the specimens were influenced by the flexural reinforcement ratio of the reinforced concrete prisms since they affect the crack width. Increments in the flexural reinforcement ratio resulted in higher strengths to concrete cone breakout;
III. The bond stress contribution in the ultimate tensile capacity of the headed anchors can be neglected for the embedment lengths tested in this research, regardless of the cracking state of the concrete;
IV. Among the theoretical methods of calculation evaluated, [1] was the one which presented the best performance, with an average of 1.42 for the ratio between the experimental and estimated strengths, showing a standard deviation of 0.36, and coefficient of variation equal to 0.25.
V. None of the methods was able to predict the exponential contribution of the flexural reinforcement ratio in the load carrying capacity of the headed anchors.
VI. The values of the factor k_1, which accounts for the cracking state of concrete, assumed in the design methods were conservative. In these tests, it grows as the flexural reinforcement ratio increases, and its values tended to be higher for lower embedment depths.

Acknowledgment

The authors wish to express their gratitude to Paul E. Regan, Emeritus Professor of the University of Westminster, for all the relevant discussions during the development of this research project. The support of CAPES, CNPq, FAP-DF and FAPESPA, Brazilian Research Development Agencies, are also acknowledged.

References

[1] American Concrete Institute (2014), "Building Code Requirements for Structural Concrete", ACI-318, New York.
[2] J. Bujnak, F. Bahleda, M. Farbak, "Headed fastenings acting in cooperation with supplementary steel reinforcement", *Procedia Engineering*, no. 91, pp. 250-255. 2014.
[3] S. C. Chun, C. S. Choi, H. S. Jung, "Side-Face Blowout Failure of Large-Diameter High- Strength Headed Bars in Beam-Column Joints", *ACI Structural Journal*, no. 114, pp. 161-172. 2017.
[4] R. Eligehausen, "Wechselbeziehungen zwischen Befestigungstechnik und Stahlbetonbauweise", (Interactions of Fastenings and Reinforced Concrete Constructions). In *Fortschritte im Konstruktiven Ingenieurbau*, Verlag Wilhelm Ernst and Sohn, Berlin. 1984.
[5] R. Eligehausen, T. Balogh, "Behavior of Fasteners Loaded in Tension in Cracked Reinforced Concrete". *ACI Structural Journal*, no. 92, pp. 365-379. 1995.
[6] R. Eligehausen, R. Mallée, J. F. Silva, "Anchorage in Concrete Construction", *Ernst & Sohn*, Berlin, Germany. 2006.
[7] R. Eligehausen, J. Ozbolt, "Influence of crack width on the concrete cone failure load", *Elsevier Applied Science*, pp. 876–881. 1992.
[8] R. Eligehausen, G. Sawade, "A fracture mechanics based description of the pull-out behavior of headed studs embedded in concrete", *Fracture Mechanics of Concrete Structures, From Theory to Applications*, London, New York, pp. 281-299. 1989.
[9] EOTA, ETAG No 001, "Anchors for use in concrete. Guideline for European Technical Approval of Metal", Brussels. 2010.
[10] fib Bulletin 58, "Design of anchorages in concrete. Fédération Internationale du Béton (fib)", Lausanne, Switzerland. 2011.
[11] G. Rehm, R. Eligehausen, R. Mallée, "Befestigungstechnik (Fixing technology)". Betonkalender, Part II, Ernst & Sohn. 1988.